

## Preparation and Characterization of UV-Cured Hybrid Coatings by Triethoxysilane-Modified Dimethacrylate Based on Bisphenol-S Epoxy

Chunguang Li, Jue Cheng, Feng Yang, Wenkai Chang, Jun Nie

State Key Laboratory of Chemical Resource Engineering, Beijing University of Chemical Technology, Beijing 100029, People's Republic of China

Correspondence to: J. Nie (E-mail: niejun@mail.buct.edu.cn)

**ABSTRACT:** Novel hybrid oligomers based on a UV-curable bisphenol-S epoxy dimethacrylate (DBSMA) were synthesized. DBSMA was modified with various amount of (3-isocyanatopropyl)triethoxysilane coupling agent. The modification degree of the hybrid oligomer was varied from 0 to 70 wt %. The photopolymerization kinetics was monitored by a real-time infrared spectroscopy. The conversion and rate of hybrid coatings increased with the increase in modification degree. UV-curable, hard, and transparent organic-inorganic hybrid coatings were prepared. They were performed by the analyses of various properties such as surface and mechanical properties. Results from the mechanical measurements showed that the properties of hybrid coatings improved with the increase in modification degree. The thermal behavior of coatings was also investigated. © 2013 Wiley Periodicals, Inc. *J. Appl. Polym. Sci.* 129: 2189–2195, 2013

**KEYWORDS:** photopolymerization; coatings; glass transition; mechanical properties; thermal properties

Received 20 July 2012; accepted 16 December 2012; published online 15 January 2013

**DOI:** 10.1002/app.38927

### INTRODUCTION

UV-curable coatings are widely used for protective purposes.<sup>1–4</sup> In the field of UV-curing industries, epoxy and epoxy acrylate derivatives have been widely used as coatings, structural adhesives, and advanced composite matrices.<sup>5</sup> For this reason, often the requirements are asked for enhanced hardness, superior thermal stability, and high gloss.<sup>6</sup> However, epoxy acrylate and derivatives does not possess adequate thermal and mechanical properties to meet the requirements of high performance structural products. Therefore, to produce surface coatings possessing particular properties, the use of monomers and oligomers containing fluorine, silicon, or phosphorus is very attractive,<sup>7–11</sup> owing to the peculiar characteristics given by these atoms presence.

The introduction of silicon compounds in the curable coatings could be promising owing to their outstanding bulk properties such as chemical and thermal and thermo-oxidative stability, flame resistance and also because they can give excellent moisture resistance and friction, weathering resistance, and excellent dielectric insulating properties.<sup>10,12,13</sup> The products containing silicon are already proposed as protective for the production of electronic devices, and the protection of optical fibers,<sup>14</sup> glass, metals, wood, and plastic. Moreover, they can also be applied as

paints for material to be used in water due to their antifouling properties.

Organic-inorganic hybrid materials offer the opportunity to combine both organic polymers (elasticity, processability) and inorganic solids (hardness, chemical inertness, and thermal resistance).<sup>15</sup> Sol-gel method was often employed to create these materials.<sup>16–20</sup> However, it would lead to potential incompatibilities (phase separation) and different stabilities of the materials.<sup>21–23</sup> So, we make chemical bonds formed between organic and inorganic polymeric systems by combining silica groups into bisphenol-S epoxy dimethacrylate (DBSMA) backbone for the formation of hybrid systems. It is expected to enhance properties, e.g., thermal properties and mechanical properties.

In our previous work,<sup>24</sup> a dimethacrylate DBSMA based on bisphenol-S (BPS) epoxy<sup>25–27</sup> was successfully synthesized. With the introduction of BPS in the skeleton, cured DBSMA exhibited higher glass transition temperature ( $T_g$ ) and better thermal stability than Bis-GMA. In this work, novel bifunctional oligomers were prepared by the reaction between DBSMA and (3-isocyanatopropyl)triethoxysilane (IPTES). The mechanical, physical, and thermal behaviors of the polymeric films obtained via the UV-curing and post-curing technique were investigated.

**Table I.** Weight Percentage Composition of the Photocurable Formulations

Sample code	Degree of modification (%)	Resin (% w/w)	Darocur 1173 (% w/w)	Viscosity (Pa-s)
MMEA-SI-0	0	98	2	12.7
MMEA-SI-10	10	98	2	8.5
MMEA-SI-30	30	98	2	5.9
MMEA-SI-50	50	98	2	3.3
MMEA-SI-70	70	98	2	1.8

## EXPERIMENTAL

### Materials

IPTES (KBE9007) was donated by ShinEtsu Company (Tokyo, Japan), 2-hydroxy-2-methyl-1-phenylpropane-1-one (1173) and benzophenone was donated by ChangZhou Runtec Chemical (Changzhou, Jiangsu, China). Ethyl-4-*N*, *N*-dimethylaminobenzoate was obtained from Aldrich (Milwaukee, WI). Di-*n*-butyltin dilaurate (DBTDL) was purchased from Beijing Chemical Reagent Company (Beijing, China). 1, 6-hexanediol dimethacrylate (HDDMA, SR239) was donated by Sartomer Company (Warrington, PA, USA). DBSMA was synthesized by reacting BPS with epichlorohydrin then with methacrylic acid in our laboratory.

### Characterization

**FTIR.** RTIR was obtained on a Nicolet 5700 instrument (Thermo Electron Corporation, Madison, WI, USA). Serie RTIR was used to determine the conversions of double bond. The blend of monomer and photoinitiator was applied between two KBr crystals and irradiated by UV spot light source (EXFO Lite, 50 W miniature ac lamp, with 5 mm crystal optical fiber, Canada) at room temperature. The light intensity on the surface of samples was 20 mW/cm<sup>2</sup> detected by UV Radiometer (Beijing Normal University, China). For each sample, the series RTIR runs were repeated three times. Because the IR absorbance was proportional to the monomer concentration, conversion-time profiles were directly obtained from the recorded curves. The double bond conversion (DC) can be expressed as follows:

$$DC(\%) = [1 - (A_t/A_0)] \times 100\% \quad (1)$$

Where  $A_0$  is the initial absorbance around 1637 cm<sup>-1</sup> and  $A_t$  is the absorbance value at irradiation time  $t$ . The polymerization rate ( $R_p$ ) was calculated from the slope of the initial linear portion of the conversion-time curves as follows:

$$\frac{R_p}{[M]_0} = \frac{d(DC)}{dt} \quad (2)$$

Where  $[M]_0$  is the initial concentration of C=C double bonds (mol<sup>-1</sup>)

**DMA.** Samples (the details are given in Table I) for dynamic mechanical analysis (DMA) were irradiated by the same UV light source for 15 min to ensure their completely curing. Mechanical properties were measured with DMA 242C

(NETZSCH, Bayern, Germany). The samples were uniform size (35 mm × 5 mm × 0.8 mm). The temperature scan was performed over a temperature range from -50 to 200°C with a ramping rate of 5°C per min (frequency of 1 Hz) by using extension mode. The loss and storage modulus, as well as the loss tangent (tanδ, ratio of loss to storage modulus), were recorded as a function of temperature. The  $T_g$  was taken to be the maximum of the loss tangent versus temperature curve.

**TGA.** The decomposition temperature of UV-cured films was measured by TA Q500 thermal analyzer at a heating rate of 10°C/min and at a test range of 30–800°C under air atmosphere. The sample weight was about 5 ± 1 mg.

**Contact Angle Measurements.** Surface static contact angles were measured with 5 μL of distilled water droplet being placed automatically on the cured film by OCA20 (Dataphysics, Stuttgart, Germany).

**Measurement of Adhesion Strength<sup>28</sup>.** Thirty micrometer thick sample was uniformly spread on the surface of glass. The dimension of one piece of glass was 50 mm × 20 mm × 5 mm. Then, the pieces of glass were overlapped in 10 mm in which the sample was spread and the bonding area was 10 mm × 20 mm. They were irradiated for 10 min under UV light with light intensity 20 mW/cm<sup>2</sup>. The samples after UV curing were tested by using a universal testing machine (Model 1185, Instron, Canton, MA, USA) with a crosshead speed of 5 mm/min at room temperature. Five samples were measured for each experiment, and the average of these values was recorded.

The volume shrinkage of novel bifunctional oligomers was measured by reflective laser beam scanning.<sup>29</sup>

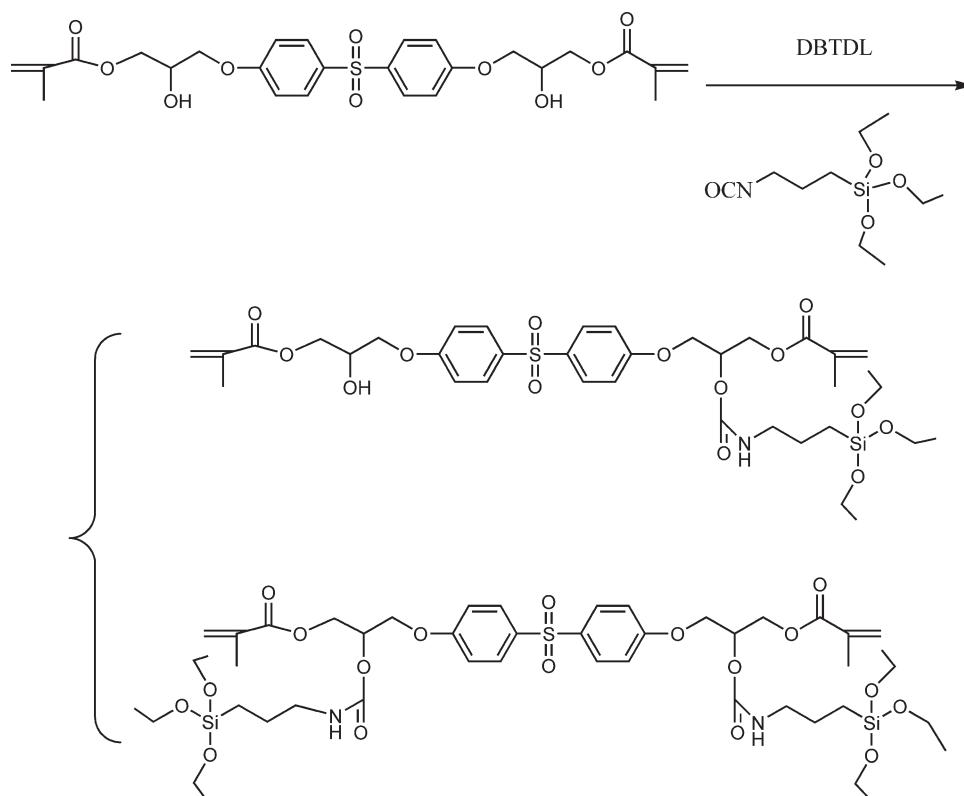
### Synthesis of Triethoxysilane-modified Dimethacrylate

As shown in Scheme 1, A mixture of 21.37 g (0.04 mol) DBSMA, 4.27 g HDDMA (80:20 DBSMA: HDDMA wt %), and 0.042 g (0.02 wt %) DBTDL was added into a 100 mL three-necked flask equipped with stirrer, thermometer, and dropping funnel. When heated to 35°C in an oil bath, 9.88 g IPTES (0.04 mol, equivalent to 50% of hydroxyl content of DBSMA) was added dropwise in 2 h, then the mixture was allowed to keep reacting for 3 h at 40°C. When the FTIR spectrum showed that the disappearance of NCO peaks at 2271 cm<sup>-1</sup>, it indicated that the reaction was finished (see Figure 1). MMEA-SI-50 was obtained.

Various feeding ratios triethoxysilane-modified dimethacrylate were synthesized according to MMEA-SI-50.

### Preparation of Hybrid Coatings

The content ratios of theoretical hydroxyl content of DBSMA and IPTES, in the liquid formulations used in the reported investigations are given in Table I. The photoinitiator (Darocur1173) concentration in these mixtures was constant and equal to 2 wt %. A thin uniform film with a layer thickness of 35 μm was coated onto glass by coater. UV curing was performed by putting the samples into the UV irradiation apparatus and cured for 5 min. After UV curing, coated plates were immersed in water at 100 °C (HCl was used as the catalyst for hydrolysis) and remained for 2 h to facilitate the hydrolysis of triethoxysilane. Then the plates were annealed at 100°C for 2 h, 130°C for



**Scheme 1.** Synthetic route of hybrid oligomers.

1 h for post-curing the silanol group. Then they were stored at room temperature for 1 day.

## RESULTS AND DISCUSSION

### Characterizations of the Synthesized Products

From 0 to 70 wt % of hydroxyl groups of DBSMA reacted with IPTES systematically to obtain triethoxysilane group via ure-

thane linkages. The  $\text{[OH]}$  group of DBSMA had a broad peak in FTIR centered at  $3484\text{ cm}^{-1}$ , and this peak gradually diminished as the reaction progressed and was replaced by a new peak corresponding to the urethane group centered at  $3380\text{ cm}^{-1}$ , the disappearance of the characteristic absorption band at  $2271\text{ cm}^{-1}$  assigned to the isocyanate group of IPTES. Structures of different modification ratio of oligomers were shown in Figure 2.

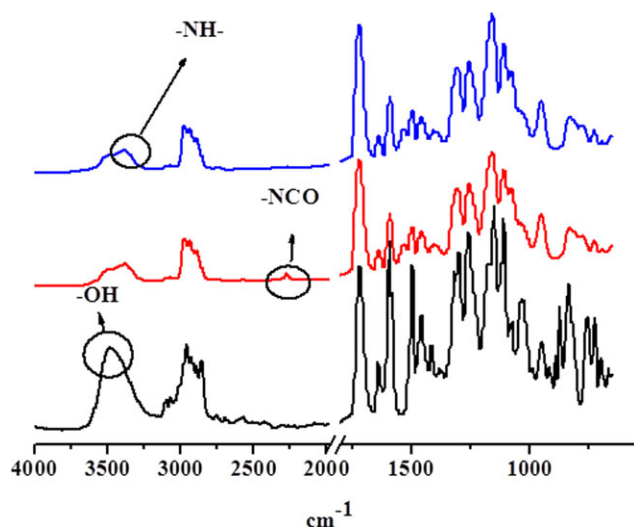


**Figure 1.** Using FTIR to monitor the process of reactions between DBSMA and (3-isocyanatopropyl)triethoxysilane. [Color figure can be viewed in the online issue, which is available at [wileyonlinelibrary.com](http://wileyonlinelibrary.com).]

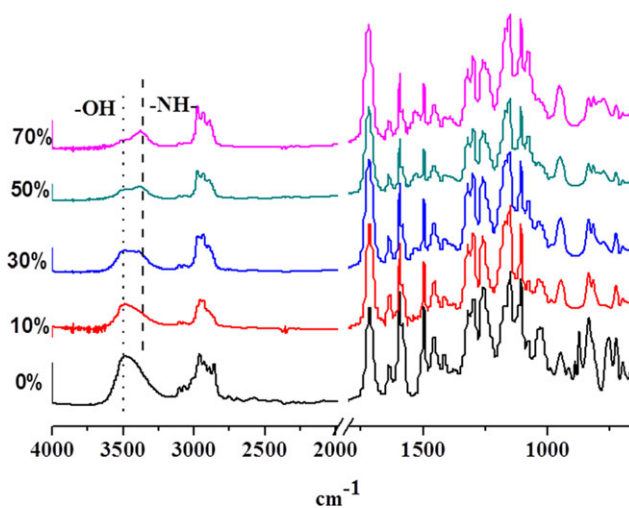


**Figure 2.** FTIR spectrum of with different modification ratio of hybrid oligomers. [Color figure can be viewed in the online issue, which is available at [wileyonlinelibrary.com](http://wileyonlinelibrary.com).]

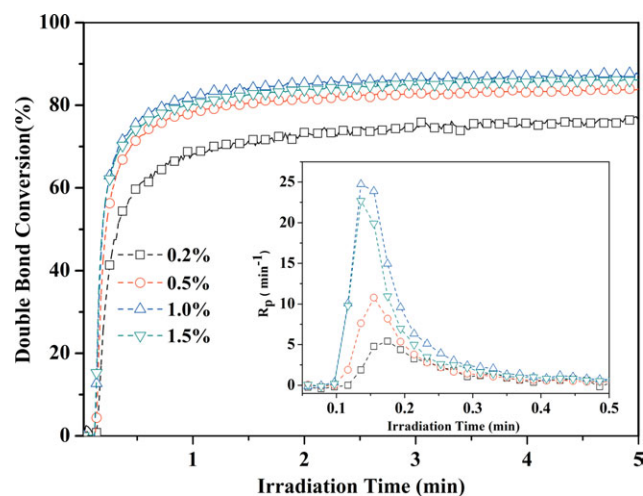


**Figure 3.** Effect of 1173 concentration on photopolymerization of MMEA-SI-50 ( $I = 20 \text{ mW/cm}^2$ ). [Color figure can be viewed in the online issue, which is available at [wileyonlinelibrary.com](http://wileyonlinelibrary.com).]

### Photopolymerization Kinetics

The concentration of the photoinitiator was a key factor to affect the photopolymerization kinetics. Optimum cure rate was generally obtained at certain concentration of photoinitiator, while further increases in photoinitiator did not produce corresponding increases in rate of cure. Figure 3 showed the DC and the rate of  $R_p$  versus the irradiation time with different concentration of Darocur1173 (0.2–1.5 wt %). It indicated that with increase of Darocur 1173, both the final  $DC_f$  (from 76.6 to 87.2%) and the maximum polymerization rate ( $(R_p^{\max})$ ) (from 5.4 to 24.7  $\text{min}^{-1}$ ) increased until it reached 1.0 wt % (high concentration photoinitiator produced more free radicals to initiate polymerization when exposed to UV light), but then decreased slightly when initiator concentration was 1.5 wt %. It might be attributed to the light absorption due to the photoinitiator when it is at high concentration: the light is screened by the initiator itself and its photolysis products.

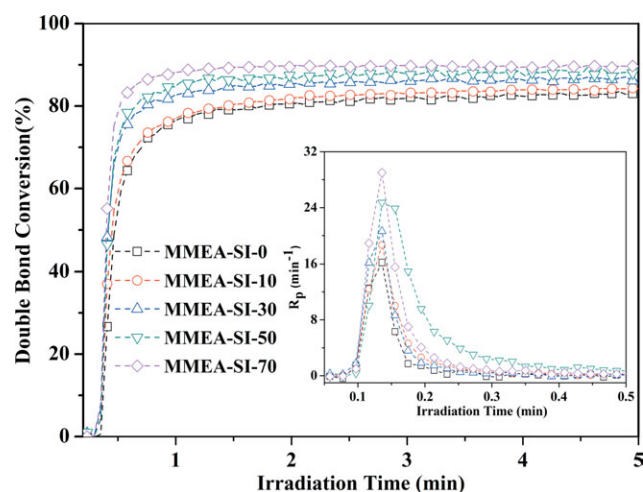


**Figure 4.** Influence of modification ratio on photopolymerization of hybrid oligomers ( $I = 20 \text{ mW/cm}^2$ ). [Color figure can be viewed in the online issue, which is available at [wileyonlinelibrary.com](http://wileyonlinelibrary.com).]

The reactivity of the UV-curable resin depends on the functionality and chemical structure of the (meth)acrylated oligomer, as well as on its viscosity, which affects the propagation and termination rate constants.<sup>30</sup> Figure 4 showed conversion and rate versus time curves for different ratio triethoxysilane-modified DBSMA exposed to UV radiation in the presence of 1 wt % 1173. The degree of vinyl conversion, determined from near infrared spectroscopy, was considerably higher for the triethoxysilane-modified DBSMA compared with DBSMA. This could be due to relatively weaker hydrogen bonding of urethane groups in the triethoxysilane-modified DBSMA (reflected in their lower viscosities) (Table I) compared to the stronger hydrogen bonding of the hydroxyl groups of DBSMA.<sup>31</sup> The increased mobility in the backbone chain in triethoxysilane-modified DBSMA thus allowed for higher  $DC_f$  and  $(R_p^{\max})$ . All eventual conversion of samples reached around 80% within 5 min.

### Dynamic Mechanical Properties

The DMA was used to investigate the thermal mechanical properties. The storage modulus ( $E'$ ) and loss factor ( $\tan\delta$ ) curves were shown in Figure 5(a,b). The temperature associated with

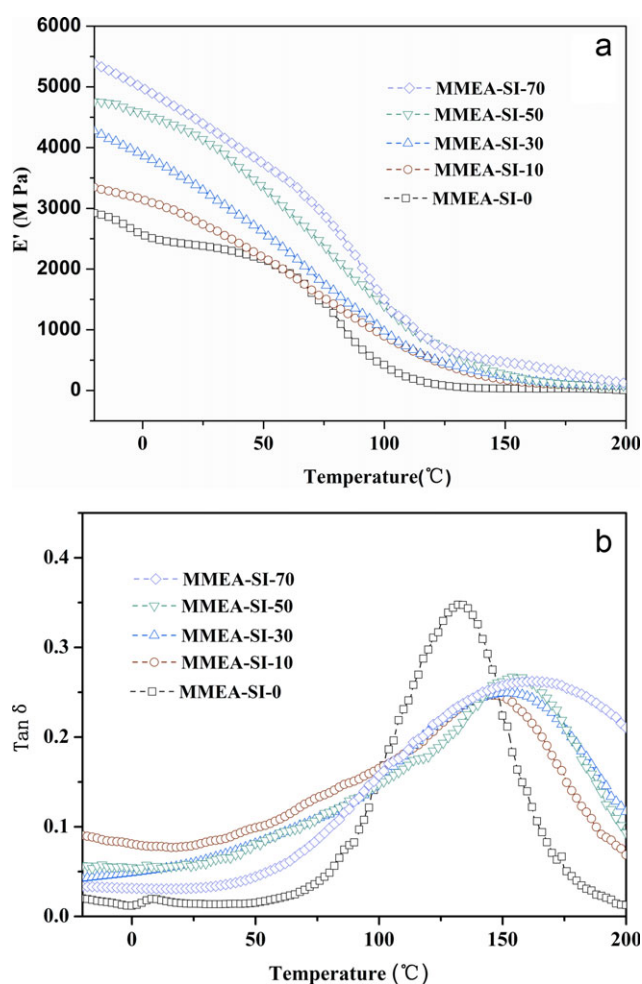


**Figure 5.** DMA curves of hybrid polymer storage modulus  $E'$  (a) and the loss factor  $\tan\delta$  (b). [Color figure can be viewed in the online issue, which is available at [wileyonlinelibrary.com](http://wileyonlinelibrary.com).]



**Table II.**  $E'$  and  $T_g$  of the UV-Cured Polymer and Hybrid Films Obtained from DMA

Sample	$E'$ at -20 ( $^{\circ}\text{C}/\text{MPa}$ )	$T_g$ ( $^{\circ}\text{C}$ )
MMEA-SI-0	2921.7	133.8
MMEA-SI-10	3346.7	144.8
MMEA-SI-30	4272.7	152.1
MMEA-SI-50	4756.3	156.2
MMEA-SI-70	5384.3	161.3

the peak position of  $\tan\delta$  curve is defined as the  $T_g$ . As the degree of modification increased from 10 to 70 wt %, the  $T_g$  increased from 133.8 to 161.3 $^{\circ}\text{C}$  (Table II). These results could be attributed to  $DC_f$  and the condensation of incorporated silanol groups which could lead to high crosslink density. High crosslink density can reduce polymer chain mobility, and, consequently, increases the  $T_g$ .<sup>32</sup> In addition, as stated above, it also enhanced the storage modulus. DMA thermograms evidenced also a  $\tan\delta$  peak broadening with modification. This is a common behavior for composites;<sup>33</sup> in addition, an increase in storage modulus above  $T_g$  in the rubbery plateau is observed with increasing degree of modification.

### Surface Properties

Table III showed the results of pendulum hardness, pencil hardness, and gloss of the films cured by UV irradiation and UV irradiation following by post-curing of silanol groups. The hardness of films was determined mainly by the crosslinking density. As seen in Table III, the pendulum hardness of sample increased gradually for the UV-curing procedure film, as the degree of modification increased. After post-curing treatment, the pendulum hardness of hybrid coatings was increased greatly and reached to the same level (around 0.93), due to the further condensation reaction between silanol groups. The hardness increase is usually related to an increase in scratch resistance, and therefore this result is particularly interesting for coating applications. The pencil hardness of coatings, which affect the abrasion and scratch resistance, depended on the chain flexibility of molecules, crosslinking density, and adhesion.<sup>34</sup> It was one of the important issues needed to be concerned. As shown in Table III, the pencil hardness was increased after the following post-curing.

Among these formulations, coating's gloss is a complex phenomenon resulting from the interaction between light and the

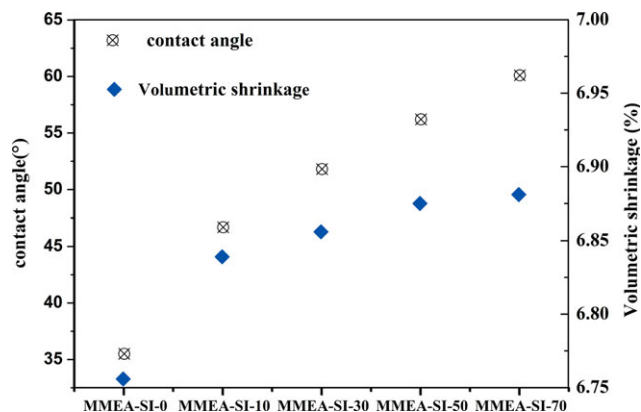


**Figure 6.** Influence of modification ratio on the water contact angles and polymerization shrinkage of UV-cured polymer. [Color figure can be viewed in the online issue, which is available at [wileyonlinelibrary.com](http://wileyonlinelibrary.com).]

surface of the coating.<sup>35</sup> The influence of post-curing on the gloss can be clearly seen. Unmodified DBSMA coatings were not affected by post-curing. After post-curing for 5 h, the gloss of MMEA-SI-10, MMEA-SI-30, and MMEA-SI-50 coatings shifted to higher values. The increased gloss may be due to the post-curing of silanol groups, which resulted in more uniform film surface. On the contrary, the gloss of MMEA-SI-70 was slightly decreasing with post-curing. This result showed that after a critical point, increasing the degree of modification diminished the gloss of hybrid coatings.

The contact angle of the UV-cured films from for MMEA-S-0 with water was around 35.1 $^{\circ}$  on the air side. When triethoxysilane-modified oligomers coated on the same substrate, i.e., glass, the wettability changed, as evidenced by the contact angle results in Figure 6. The contact angle measured on the air side clearly depends on the silicon-containing concentration. The contact angle of the UV-cured films containing silicon increased extensively in the film, to 60.8 $^{\circ}$  in the MMEA-SI-70 film. A medium polarity surface was formed, containing hydrophobic groups (the silicon) together with the polar groups of acrylic oligomer, such as sulphone and hydroxy.<sup>36</sup> Those results may be explained that on the air side the content of silicon is much higher than expected on the basis of the film composition.<sup>37</sup> A silicon-containing molecule triethoxysilane contains only one silicon atom, so it cannot obtain a complete hydrophobic surface.

**Table III.** Surface Properties of Hybrid-Cured Films

		MMEA-SI-0	MMEA-SI-10	MMEA-SI-30	MMEA-SI-50	MMEA-SI-70
Pendulum hardness	UV curing	0.861	0.875	0.889	0.890	0.889
	Post curing (5 h)	0.861	0.911	0.920	0.930	0.927
Pencil hardness	UV curing	6H	6H	6H	6H	6H
	Post curing (5 h)	6H	7H	7H	8H	8H
Gloss	UV curing	178	183	185	192	192
	Post curing (5 h)	178	187	190	193	192

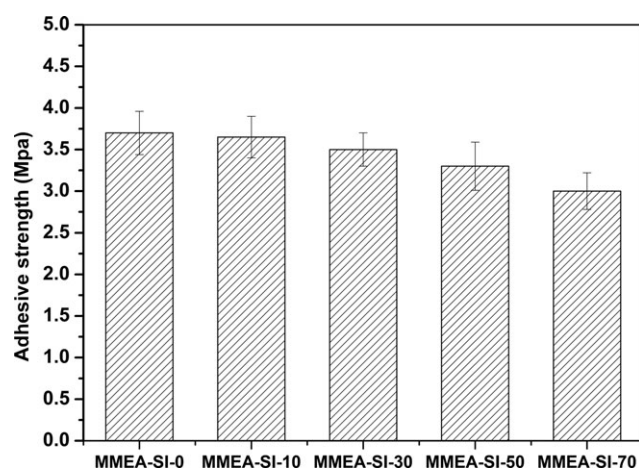


**Figure 7.** Influence of modification ratio on adhesive strength of hybrid coatings.

### Adhesive Strength

In general, the adhesive strength at the interface was decided by three factors: specific interaction like electrostatic interaction (hydrogen bond and vander Waals force), effect of polymerization shrinkage, and other factors (an anchor effect at the interface). The result of adhesive was shown in Figure 7. Adhesion strength was decreased along with the increase of modification degree. The contact angle value of uncoated glass plates was 33.8°. The uncoated glass plates have a fairly polar surface. The hydrophilicity of uncoated glass plates and of the unmodified coating was close to each other. Triethoxysilane made the surface of coating more hydrophobic. Moreover, Polymerization shrinkage of the triethoxysilane-modified DBSMA was higher than DBSMA due to their higher conversion compared to the DBSMA (see Figure 7). Therefore, it was assumed that that the surface polarity and polymerization shrinkage were responsible for the poor adhesion.

### Thermal Stabilities

The thermal stability of the hybrid systems was determined using a thermogravimetric analyzer. The TGA curves of MMEA-SI-0 and in the presence of increasing degree of modification (from room temperature to 800°C in air atmosphere) were shown in Figure 8. The specific degradation temperatures and the final char yields at 800°C were listed in Table IV. These data indicated that with increasing amount of modification in the photocurable formulation, the thermal stability of the hybrid

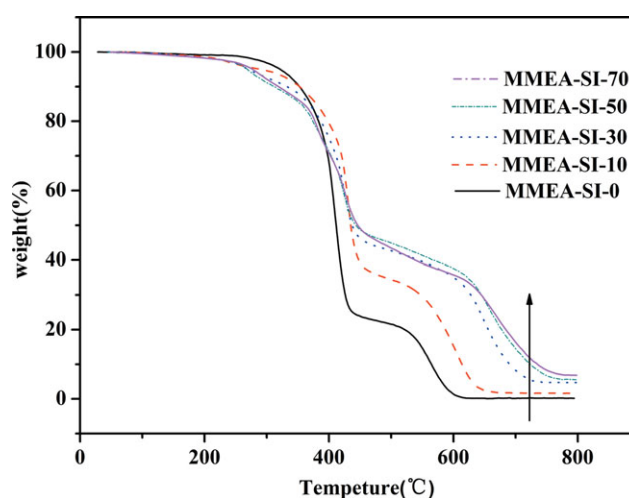


**Figure 8.** TGA curves of the cured films with different modification ratio under air flow. [Color figure can be viewed in the online issue, which is available at [wileyonlinelibrary.com](http://wileyonlinelibrary.com).]

network was enhanced. The hybrid materials also showed a higher char content or reduced weight loss at 800°C with degree of modification increasing. While MMEA-SI-0 network showed a char content of 0.17%, in the presence of 10 wt % degree of modification, the char content increased to a value of 1.62% and reached 6.8% in the cured film obtained in the presence of 70 wt % degree of modification. These char content values were in good agreement with the theoretical content of silica and used as a preliminary indicator of flame resistance.

### CONCLUSIONS

UV-curable hybrid systems were prepared through a dual cure process, which involved first the photopolymerization of oligomers and then hydrolysis and subsequent condensation of alkoxy silane groups. The conversion and rate of hybrid oligomers increased with the increase in modification degree. Evident hardness and gloss increase were obtained in the hybrid systems. The  $T_g$  values and storage modulus of the hybrid films increased with the increase of the triethoxysilane-modified degree. The thermal stability of hybrids at high temperature was also higher than that of the pure oligomer resin. However, the adhesion of coating onto the glass substrate was poor.

**Table IV.** TGA Data of Hybrid-Cured Films

Sample	Temperature at the certain weight loss (°C)					Residue (%) (800 °C)
	10%	30%	50%	70%	90%	
MMEA-SI-0	353.1	397.9	411.9	426.6	564.5	0.17
MMEA-SI-10	352.1	420.3	435.0	547.0	613.5	1.62
MMEA-SI-30	332.1	411.2	437.8	627.5	689.8	4.68
MMEA-SI-50	311.8	404.2	442.7	645.0	723.4	5.52
MMEA-SI-70	318.1	402.0	446.2	644.3	734.6	6.80

REFERENCES

1. Chattopadhyay, D.; Panda, S. S.; Raju, K. *Prog. Org. Coat.* **2005**, *54*, 10.
2. Kardar, P.; Ebrahimi, M.; Bastani, S.; Jalili, M. *Prog. Org. Coat.* **2009**, *64*, 74.
3. Roşu, D.; Ciobanu, C.; Caşcaval, C. *Eur. Polym. J.* **2001**, *37*, 587.
4. He, Y.; Zhou, M.; Wu, B.; Jiang, Z.; Nie, J. *Prog. Org. Coat.* **2010**, *67*, 264.
5. Bayramoğlu, G.; Kahraman, M. V.; Kayaman-Apohan, N.; Güngör, A. *Polym. Adv. Technol.* **2007**, *18*, 173.
6. Bayramoğlu, G.; Kahraman, M. V.; Kayaman-Apohan, N.; Güngör, A. *Prog. Org. Coat.* **2006**, *57*, 50.
7. Ni, Y.; Zheng, S.; Nie, K. *Polymer* **2004**, *45*, 5557.
8. Chiang, C. L.; Ma, C. C. M.; Wang, F. Y.; Kuan, H. C. *Eur. Polym. J.* **2003**, *39*, 825.
9. Xu, F.; Yang, J. L.; Gong, Y. S.; Ma, G. P.; Nie, J. *Macromolecules* **2012**, *45*, 1158.
10. Liu, Y. L.; Chiu, Y. C.; Wu, C. S. *J. Appl. Polym. Sci.* **2003**, *87*, 404.
11. Grunlan, M. A.; Lee, N. S.; Cai, G.; Gädda, T.; Mabry, J. M.; Mansfeld, F.; Kus, E.; Wendt, D. E.; Kowalke, G. L.; Finlay, J. A. *Chem. Mater.* **2004**, *16*, 2433.
12. Tang, C.; Liu, W. *J. Appl. Polym. Sci.* **2010**, *117*, 1859.
13. Wang, X.; Hu, Y.; Song, L.; Xing, W.; Lu, H. *J. Polym. Sci., Part B: Polym. Phys.* **2010**, *48*, 693.
14. Wang, P.; Schaefer, D. W. *Langmuir* **2008**, *24*, 13496.
15. Chiang, H. C.; Liu, C. H.; Tsiang, R. C. C. *J. Polym. Sci., Part A: Polym. Chem.* **2008**, *46*, 8149.
16. Judeinstein, P.; Sanchez, C. *J. Mater. Chem.* **1996**, *6*, 511.
17. Zou, J.; Shi, W.; Hong, X. *Comp. Part A: Appl. Sci. Manufact.* **2005**, *36*, 631.
18. Sangermano, M.; Malucelli, G.; Amerio, E.; Priola, A.; Billi, E.; Rizza, G. *Prog. Org. Coat.* **2005**, *54*, 134.
19. Schmidt, H.; Jonschker, G.; Goedicke, S.; Mennig, M. *J. Sol-Gel Sci. Technol.* **2000**, *19*, 39.
20. Crivello, J. V.; Mao, Z. *Chem. Mater.* **1997**, *9*, 1554.
21. Kickelbick, G. *Prog. Polym. Sci.* **2003**, *28*, 83.
22. Choi, J.; Yee, A. F.; Laine, R. M. *Macromolecules* **2003**, *36*, 5666.
23. Wu, C. C.; Hsu, S. L. C. *J. Phys. Chem. C* **2010**, *114*, 2179.
24. Li, C.; Cheng, J.; Jian, Y.; Chang, W.; Nie, J. *J. Appl. Polym. Sci.* **2012**. DOI: 10.1002/app.37511.
25. Park, S. J.; Jin, F. L. *Polym. Degrad. Stab.* **2004**, *86*, 515.
26. Liaw, D. J.; Shen, W. C. *Die Angewandte Makromolekulare Chemie* **1992**, *199*, 171.
27. Chiu, Y. C.; Chou, I.; Tseng, W. C.; Ma, C. C. M. *Polym. Degrad. Stab.* **2008**, *93*, 668.
28. Li, H.; Niu, R.; Yang, J.; Nie, J.; Yang, D. *Carbohydr. Polym.* **2011**, *86*, 1578.
29. Jian, Y.; He, Y.; Jiang, T.; Li, C.; Yang, W.; Nie, J. *J. Polym. Sci., Part B: Polym. Phys.* **2012**, *50*, 923.
30. Decker, C. *Prog. Polym. Sci.* **1996**, *21*, 593.
31. Khatri, C. A.; Stansbury, J. W.; Schultheisz, C. R.; Antonucci, J. M. *Dent. Mater.* **2003**, *19*, 584.
32. Cheng, X.; Liu, S.; Shi, W. *Prog. Org. Coat.* **2009**, *65*, 1.
33. Crivello, J. V.; Acosta Ortiz, R. *J. Polym. Sci., Part A: Polym. Chem.* **2002**, *40*, 2298.
34. Mülazim, Y.; Kahraman, M. V.; Apohan, N. K.; Kızıldaş, S.; Güngör, A. *J. Appl. Polym. Sci.* **2011**, *120*, 2112.
35. Wu, S.; Sears, M. T.; Soucek, M. D. *Prog. Org. Coat.* **1999**, *36*, 89.
36. Huo, L.; Gao, J.; Zhang, X. *J. Appl. Polym. Sci.* **2009**, *113*, 3693.
37. Batten, R.; Davidson, R.; Ellis, R.; Wilkinson, S. *Polymer* **1992**, *33*, 3037.